NIGERIAN JOURNAL OF ENGINEERING RESEARCH UNICROSS (NJERU)

Volume 1, Issue 2, 1st June, 2024

# Design And Optimization of Three Phase Induction Motor for Transport Application

Ephraim Bassey Ekpenyong[a*], Gertrude Fischer[b], Asuquo Eke[c]

[a,b,c] Department of Electrical Electronic Engineering, Faculty of Engineering, University of Cross River State, Calabar, Nigeria.

[*]Corresponding author: Email: ephraims202@gmail.com

Received: 20th September, 2024 Reviewed: 23rd October, 2024 Accepted: 30th October, 2024

**ABSTRACT**

The growing demand for sustainable and energy-efficient transportation systems has driven the need for advanced electric motor technologies. Three-phase induction motors (TPIMs), known for their robustness and cost-effectiveness, are gaining attention as a viable alternative to permanent magnet motors (PMMs) in transport applications. However, TPIMs face several challenges in meeting the specific requirements of transportation systems, including compact size, lightweight construction, and high torque performance under dynamic load conditions. This study aims to design and optimize TPIMs for electric vehicles and other transport systems, focusing on improving efficiency, reducing energy losses, and enhancing thermal performance. A comprehensive design framework will be developed, integrating electromagnetic modelling and thermal management strategies, with a focus on sustainable material selection to reduce environmental impact. Advanced optimization techniques, such as genetic algorithms optimization, was applied to balance key design objectives, including efficiency, cost, and power density. Simulation and experimental validation were conducted to assess the practical applicability of the optimized designs. The results of this study showed that three phase induction motors when modelled and optimized, they are more efficient, sustainable, and cost-effective in transportation, supporting the transition to cleaner, electrified transportation systems as shown in the plotted figures of the result.

**Keywords**: Design, Modelling, Optimisation, Three-phase Induction Motor, Rotor Bars, Transportation systems

## INTRODUCTION

The transportation sector is undergoing a significant transformation due to the global push for sustainable and energy-efficient solutions. Electric propulsion systems have emerged as a critical component in this transition, with electric motors at the heart of these systems. Among the various motor technologies available, three-phase induction motors (TPIMs) have historically been utilized in industrial applications due to their robustness, reliability, and cost-effectiveness (Smith & Johnson, 2020). However, their adoption in transportation, particularly for electric vehicles (EVs), trains, and buses, is gaining traction as a viable alternative to permanent magnet motors (PMMs), (Johnson & Lee 2019).

Three-phase induction motors are characterized by their simple construction, low maintenance requirements, and ability to operate efficiently in harsh environments. Unlike PMMs, which rely on rare-earth materials, TPIMs are free from such dependencies, making them a more sustainable and environmentally friendly option, Williams, (2022). However, TPIMs face challenges in achieving comparable power density and efficiency levels to PMMs, especially in transport applications where compact design, lightweight construction, and high torque performance are critical, Chen & Zhao, (2019, 2022).

The transportation sector also introduces unique operational challenges, such as dynamic load profiles, frequent speed changes, and strict space and weight constraints. These demands necessitate advanced design and optimization approaches for TPIMs, including the use of computational methods to improve energy efficiency, thermal management, and electromagnetic performance, Kumar et al., (2020a, b). Moreover, integrating recyclable materials and innovative manufacturing techniques is essential to meet sustainability goals, Bose et al., (2022).

Despite their potential, research on TPIMs for transportation applications remains limited compared to other motor technologies. Existing studies often focus on industrial use cases, leaving a gap in the development of TPIMs specifically tailored for transport systems, Rao et al., (2022). Addressing this gap requires interdisciplinary efforts to optimize motor design, incorporating advanced algorithms, thermal model ling, and material innovations. This study aims to bridge these gaps by advancing the design and optimization of TPIMs for transportation, contributing to the global shift toward electrified and sustainable transport systems.

## Materials and Methods

### A. Materials

*Electromagnetic Materials:*

i. Copper: Used for windings due to its excellent electrical conductivity.
ii. Steel: Typically used for the core due to its magnetic properties.
iii. Laminated Steel Sheets: Reduce eddy current losses in the core.

*Insulating Materials:*

i. Epoxy Resins: Used for insulating the windings.
ii. Insulating Tapes: Applied to ensure electrical insulation between windings.

*Cooling Materials:*

i. Coolants (e.g., water-glycol mixture): Used for cooling systems to manage the thermal performance.
ii. Heat Sinks and Fans: To dissipate heat generated during operation.

*Composites and Advanced Materials:*

i. Carbon Fiber Composites: For lightweight and strong structural components.
ii. Nanomaterials: For enhancing the magnetic and electrical properties of core and winding materials.

*Software and Tools:*

i. Finite Element Analysis (FEA) Software: For modeling and simulating the electromagnetic properties and performance (Ansys).
ii. Thermal Analysis Software: To simulate and optimize the thermal management system (ANSYS).
iii. Mathematical Computing Software: For solving differential equations and optimizing motor designs (MATLAB).

*Mechanical Components:*

i. Bearings: To ensure smooth rotation and reduce friction.
ii. Shafts: Made of high-strength steel to transmit mechanical power.
iii. Frames and Housings: For supporting and protecting the motor components.

*Instrumentation and Testing Equipment:*

i. Oscilloscopes and Multimeters: For measuring electrical parameters during testing.
ii. Dynamometers: For testing the mechanical performance of the motor.
iii. Thermocouples and Thermal Cameras: To monitor and analyze the thermal performance.

The following materials were used for this work. i.) Three Phase Induction Motor Rotor Bars, ii, Induction Motor Rotor Bars Data, iii) MATLAB/Simulink Apps, iv) Ansys Maxwell 2D tools

### B. *Method*

The design and optimization of three-phase induction motors for transport applications involve a systematic process that begins with defining specific requirements such as power output, torque, speed, and efficiency. Advanced modeling and simulation techniques, including finite element analysis (FEA), to predict the motor's performance and optimize design parameters for electromagnetic, thermal, and mechanical aspects. This is followed by the creation of detailed 3D models and simulations to refine the motor's performance. Once the initial design is optimized, a prototype is developed and subjected to rigorous testing to validate its performance under various conditions. The test results are analyzed to identify any discrepancies, and necessary design adjustments are made in an iterative cycle until the motor meets all the desired criteria. After extensive validation and compliance testing, the final design is documented and reported, summarizing the entire process and providing recommendations for further studies. The selected motor parameters were then optimized for transport applications using MATLAB tools.

### C. *Model Equations*

*Electrical Equation*

Armature Circuit

$$\frac{dia}{dt} = \frac{Va - Raia - Kbwmif}{La} \quad 1$$

*Where*: ia = the armature current, Va = the armature voltage, Ra = the armature resistance, La = the armature inductance, Kb = the back EMF constant, ωm = the mechanical angular speed, if = the field current

Field Circuit:

$$\frac{dif}{dt} = \frac{Vf - Rfif}{Lf} \quad 2$$

Where: Vf = the field voltage, Rf = the field resistance, Lf = the field inductance

*Mechanical Equation*

Mechanical Dynamics:

$$\frac{dwm}{dt} = \frac{Te - Bwm - Tl}{J} \quad 3$$

Where: ωm = the mechanical angular speed, Te = the electromagnetic torque, B = the friction coefficient, Tl = the load torque, J = the moment of inertia

Electromagnetic Torque:

$$\text{Te} = Kbiaif \quad 4$$

Where: Te = the electromagnetic torque, Kb = the torque constant, ia = the armature current, if = the field current.

Optimization model equations

*Maximize Efficiency (η)*

$$\boldsymbol{\eta} = \frac{\boldsymbol{Pout}}{\boldsymbol{Pin}} \quad \mathbf{5}$$

Where: Pout = the output power, Pin = the input power

*Minimize Weight (W)*

W=∑(Density × Volume) of all motor components

*Minimize Cost (C)*

C=∑(Cost per unit volume × Volume) of all motor components

*Electromagnetic Constraints:*

$B_{max} \leq B_{limit}$ (Maximum flux density)

$J_{max} \leq J_{limit}$ (Maximum current density) 6

Where: $B_{max}$ is the maximum flux density, $B_{limit}$ is the allowable flux density, $J_{max}$ is the maximum current density≤ $J_{limit}$ is the allowable current density

*Electromagnetic Torque Equation (Objective and Constraint)*

$$\text{Te} = \text{k}\cdot\phi\cdot\text{Ir} \quad 7$$

Where:

Te = the electromagnetic torque, k = a constant specific to the motor design, ϕ = the magnetic flux, Ir = the rotor current

### C. *Model Process of Three Phase Induction Motor in Ansys Maxwell*

Figure 1 presents the overall machine model showing the total overview of the modelled motor. It displays the major parametric components such as the stator, rotor, shaft, stator slot and rotor slot. All the dimensions are done in millimetres. The rated voltage and rated speed were inclusive.

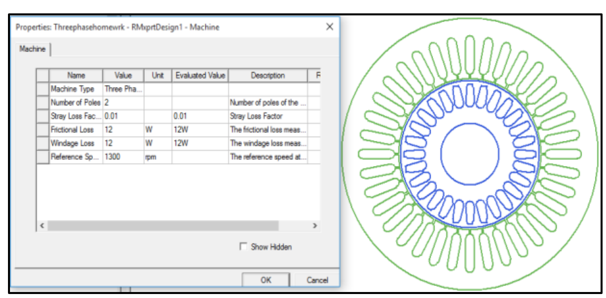


Figure 1. OVERALL MACHINE MODEL

The figure 2. presents a stator model, is the designing process for the stator of the selected motor. The stator has the following parameters, outer diameter, inner diameter, length, steel type, slot type amongst others. All the dimensions were taken in millimetres.

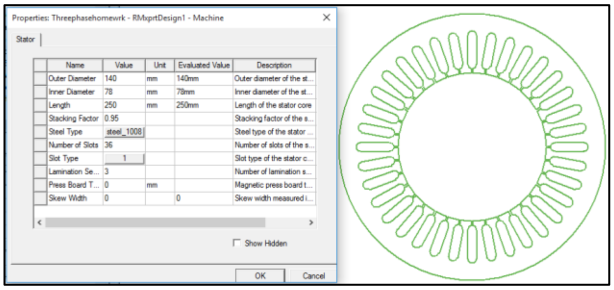

Figure 2. STATOR MODEL

Figure 3. presents the stator slot model, it shows the slot at the stator. It has dimensions such as Hs0, Hs2, Bs0, Bs1, Bs2. All the dimensions are taken in millimetres.

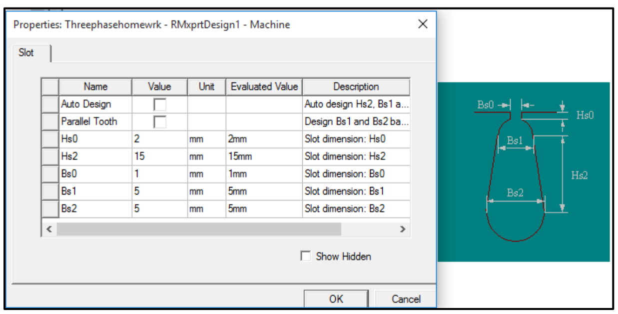


Figure 3. STATOR SLOT MODEL

Figure 4. presents the stator winding model, it shows the winding model of the stator. It has two winding layers, whole coil type, one parallel branch, and capacity of thirty conductors, amongst others. The total number of winding slots was 32 with equal air gap.

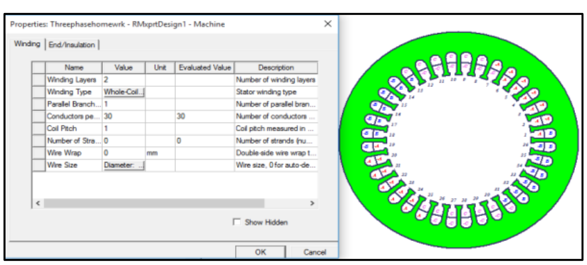

Figure 4. STATOR WINDING MODEL

Figure 5. presents the stator winding distribution model, it shows the winding distribution within the stator windings with winding sequence of A, B & C and –A, -B & -C respectively.

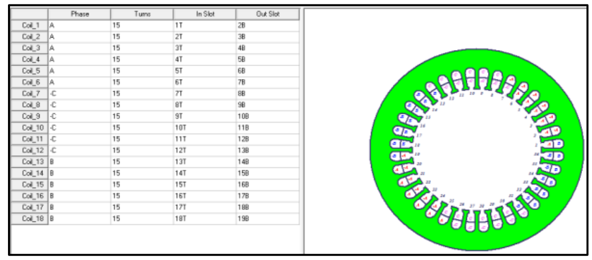

Figure 5. STATOR WINDING DISTRIBUTION MODEL

Figure 6. presents the stator model, is the designing process for the rotor of the selected motor. The stator has the following parameters, outer diameter, inner diameter, length, steel type, slot type amongst others. All the dimensions were taken in millimetres.

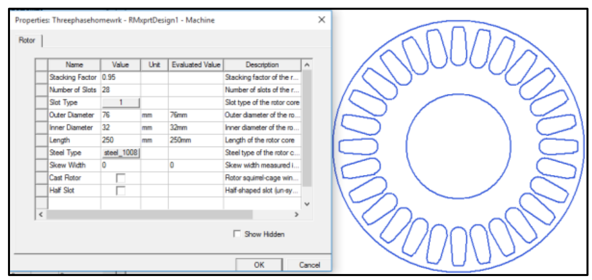

Figure 6. ROTOR MODEL

Figure 7. presents the stator slot model, it shows the slot at the rotor. It has dimensions such as Hs0, Hs1, Hs2, Bs0, Bs1, Bs2. All the dimensions are taken in millimetres.

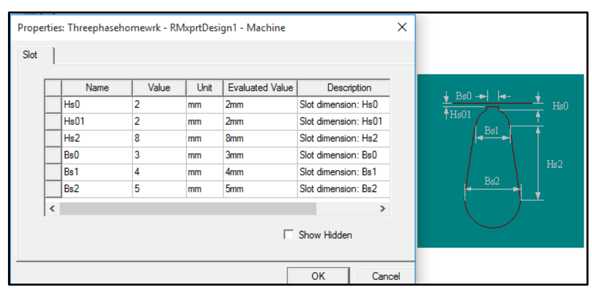


Figure 7. ROTOR SLOT MODEL MODEL

Figure 8. presents the stator model, is the designing process for the rotor of the selected motor. The stator has the following parameters, outer diameter, inner diameter, length, steel type, slot type amongst others. All the dimensions were taken in millimetres.

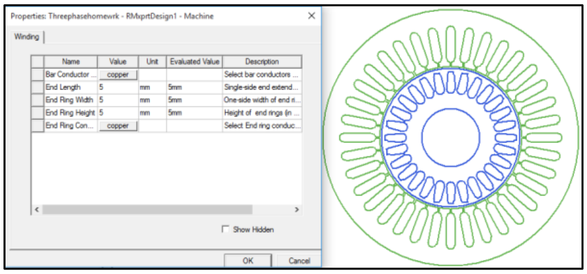

Figure 8. ROTOR WINDING MODEL

## Results and Discussion

### *Prediction Outcome*

Figure 9. presents the phase current output in RMXPrt interface, it showed the motor phase current performance during simulation. Starting at point of origin 0.00A, the motor phase current built up and progressed to an all-time high of 82.50A at a corresponding motor speed of 3000rpm. This motor system output with respect to the speed tallies with the reference speed of the selected motor in question. Since this built up current in the motor's phase was less than 100A, it implied that the motor was performing at its safety region when applied in transportation system.

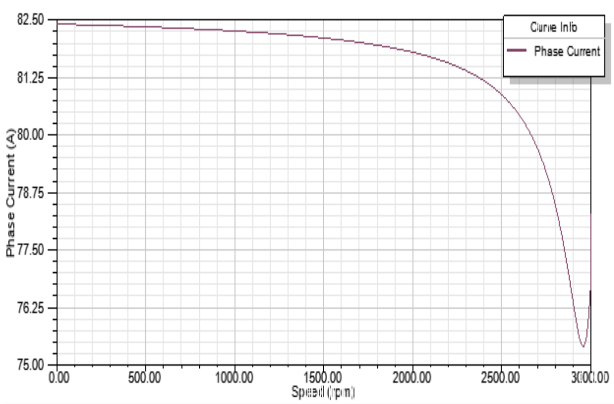


Figure 9. PHASE CURRENT OUTPUT

Figure 10. presents the RMXPrt interface for stator efficiency output in Figure 2, showed the selected motor efficiency performance when modeled for transport applications. At the origin point of 0.00%, the motor runs at a constant speed of 500rpm and then began to vary due to different loading conditions. The efficiency of the motor progressed to a maximum of 6% at a corresponding speed of 3000rpm. This efficiency is a product of 102. This level of efficiency is ideal for transport applications of the three-phase induction motor.

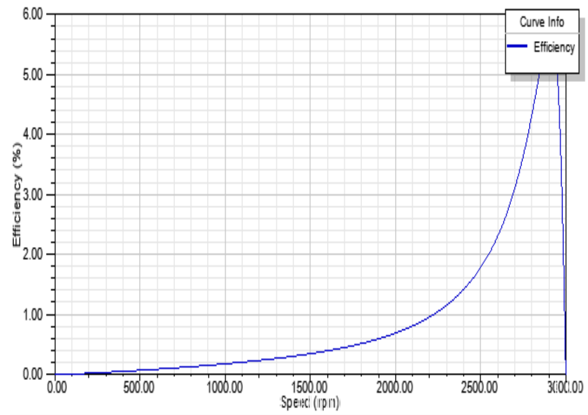


Figure 10. STATOR EFFICIENCY POWER

Figure 11. presents the RMXPrt interface for stator output power in figure 3, showed the selected motor output power performance when modeled for transport applications. At the origin point of 0.00%, the motor runs at a constant speed of 500rpm and then began to vary due to different loading conditions. The output power of the motor progressed to a maximum of 1500W at a corresponding speed of 3000rpm. This output power is a product of $10^3$. This level of output power is ideal for transport applications of the three-phase induction motor. It can withstand sudden fluctuations in the system.

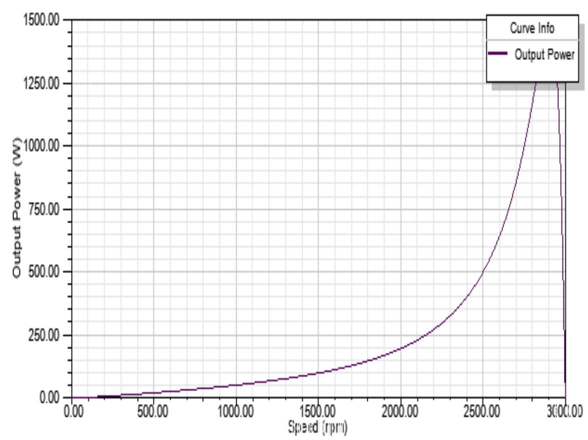


Figure 11. STATOR OUTPUT POWER

Figure 12. presents the running torque output, it indicated the output torque performance of the selected motor while in operation. Recalling that in three phase induction motor, torque of the motor is a critical

component for it deploy ability and functionality to its maximum capacity. At a reference speed maximum of 3000rpm, the motor torque rose from 0.50N-m and progressed to a maximum peak of 4.00N-m. This torque is a measure of 103. This is the required torque to run this motor in the RMXPrt interface which was then transferred to the 2D interface to really correspond with the needed field experience.

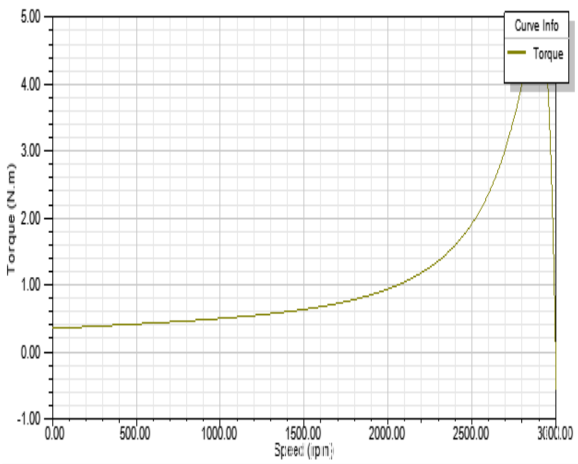


Figure 11. RUNNING TORQUE OUTPUT

Figure 13. presents the rotor efficiency, it showed the efficiency during the RMXPrt interface of the rotor as the motor was under the influence of full excitation. This efficiency helps the simulation process to understand the variations between the rotor and shaft and the stator influence. This is mostly affected by the loading and offloading process of the motor. Most applicably in the transport system whereby passengers are never a fixed load. They onboard and disembark with no specific time, speed and distance. Thus, for the motor to continue serving its modelling purpose, this efficiency must not drop.

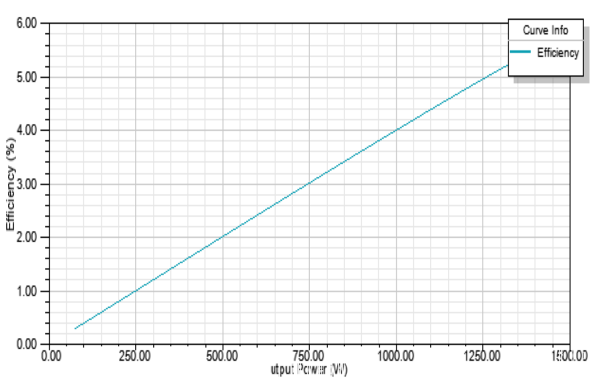


Figure 13. ROTOR EFFICIENCY

Figure 14. presents the motor slip, this is shown in the RMXPrt interface. Corresponding to the motor's torque performance is the slip with no reference unit. This happens at the maximum reference power of 1500W. During this point, the slip was maximum at 3%. This point of 0.030 maximizes the overall performance of the motor when modeled with keen interest in transport applications. This specific characteristic makes it more resilient to fluctuations and maintains good torque at both starting and running.

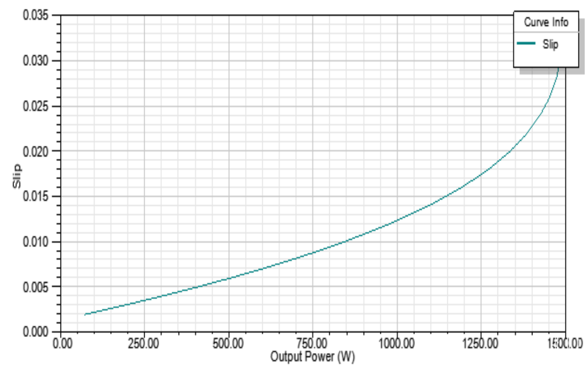


Figure 13. MOTOR SLIP

Figure 14. presents the motor reactance in the RMXPrt interface, it showed the three characteristics of the rotor performance when loaded under transient. First is the rotor leakage reactance x1 which indicates what happened within the stator when the motor is excited and flux are generated. Some excess of the flux, tends to leak out of the winding's confinement. Secondly, the rotor resistance r2, is another serious point of consideration in the formation process of this model. It represents the losses component within the windings of the motor. If this is not carefully handled, it could lead to serious thermal disorder in the motor that may adversely affects its performance in terms of output and stability especially when used in transport applications. The third components of this result are the rotor leakage reactance x2 which demonstrates the effect of the flux flow as generated within the rotor of the motor windings. During this process, some amount of the flux tends to stray way from the winding confinement and they are termed leakage flux leading to rotor leakage reactance. When this motor is used for transport purpose, these reactance and resistance in the rotor helps to ensure balance between the internal and external environment of the selected motor.

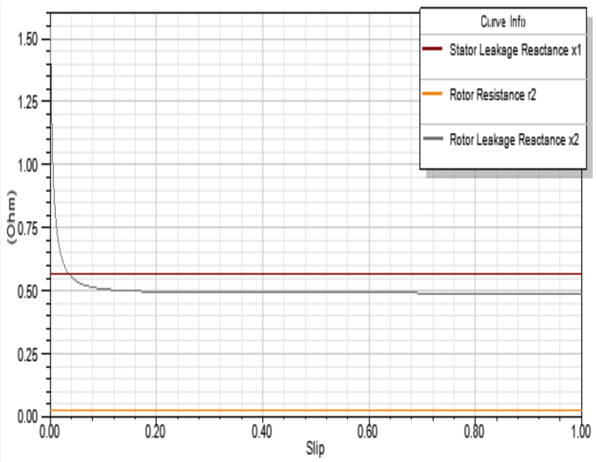


Figure 14. MOTOR REACTANCE

Figure 15 presents The RMXPrt interface for rotor output power. It showed the selected motor output power performance when modelled for transport applications. At the origin point of 0.00%, the motor runs at a constant speed of 9000rpm and then began to vary due to different loading conditions. The output power of the motor progressed to a maximum of 1000W at a corresponding speed of 9000rpm. This output power is a product of 103. This level of output power is ideal for transport applications of the three-phase induction motor. It can withstand sudden fluctuations in the system.

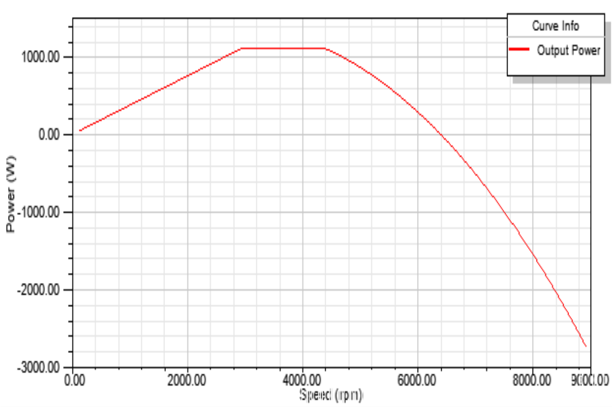


Figure 15. Rotor OUTPUT POWER

Figure 16. presents torque performance with transport application; it showed the skewed behaviour of the selected motor torque with respect to time. The characteristic of this torque indicated that for a three-phase motor of 15kW, the starting torque is low but with an increased running torque. This is a good development if applied in a transport system whereby distances and demographics differs as well as the variation in the magnitude of the load applied. For a sustainable transport system application with this model, it is necessary to vary the time but a constant torque be maintained as shown here.

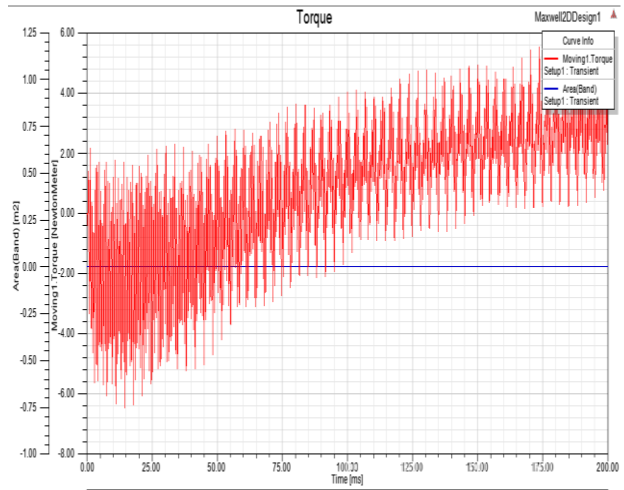


Figure 16. TORQUE PERFORMANCE WITH TRANSPORT APPLICATION

Figure 17 presents the torque performance with heavy duty transport application. This shows the response of the motor torque when applied to heavy duty in transport system. The characteristic of this torque indicated that for a three-phase motor of 125kW, the starting torque is low but with an increased running torque. This is a good development if applied in a transport system whereby distances and demographics differs as well as the variation in the magnitude of the load applied. For a sustainable transport system application that would include heavy duty with this model, it is necessary to vary the time but a constant torque be maintained as shown here.

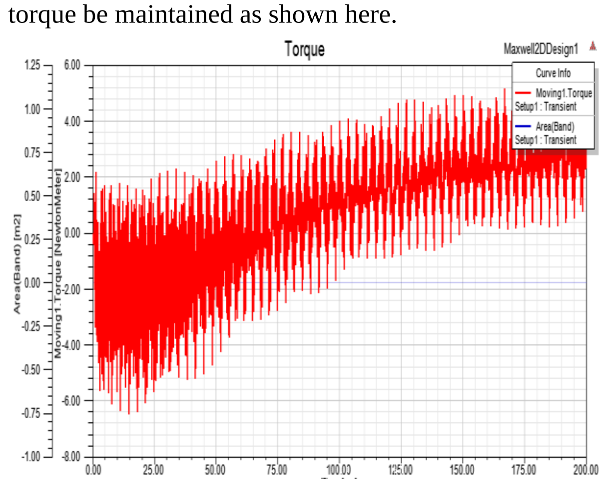


Figure 17. TORQUE PERFORMANCE WITH HEAVY DUTY TRANSPORT APPLICATION

In Figure 18 presents the simulated phase currents, it showed the combined three phase current windings. These phases are phase A, B and C. Phase A is denoted with red, phase B is grey and phase C is blue. From the origin, phase A started, while phase B and phase C all started at the +50.00 and -50.00A and all the three phases progressed sinusoidally with a maximum time of lapse of 200.00sec. The maximum current magnitude was +120.00A and -120.00A respectively. This performance of the motor phases current occurred during its transient. For application in transport system, 120.00A current is good enough to run the motor for maximum torque, efficiency and output power.

In Figure 19. Presents the simulated phase A current, this shows the performance of phase A picked out of the three phases of the selected motor. A uniform display indicates the operational stability of the motor when used for transport application. Thus, it is dependable and welcoming.

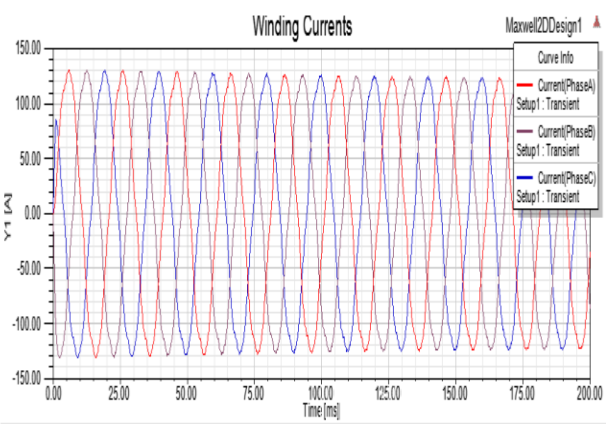


Figure 18. SIMULATED PHASE CURRENTS

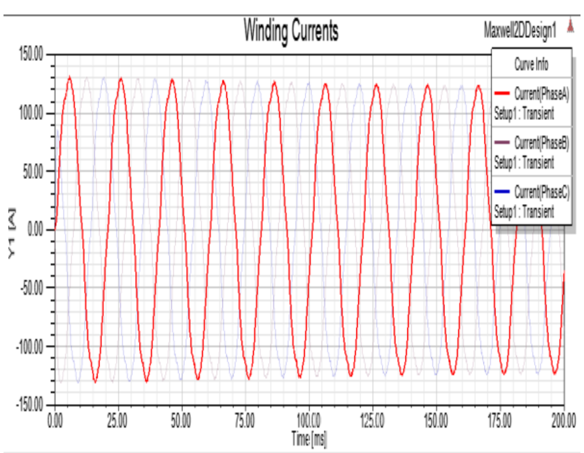


Figure 19. SIMULATED PHASE A CURRENTS

Figure 20. presents the simulated phase B current, this shows the performance of phase B picked out of the three phases of the selected motor. A uniform display indicates the operational stability of the motor when used for transport application. Thus, it is dependable and welcoming.

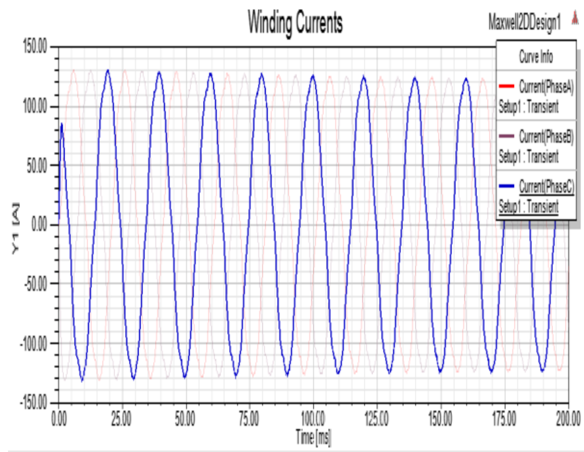


Figure 20. SIMULATED PHASE C CURRENTS

Figure 21. presents the simulated motor core losses. As the three phase induction motor is model to fit into the transport system, during operations, the motor will develop heat, wear and tear but the core losses that occurs at the inner part of the motor are more worrisome. This is from the stator and rotor windings. In this result, it can be observed that the motor losses were minimal. At transient, the core losses were almost zero and during loads, the core losses were just 0.0015W. Thus, this model can fit into the transport as modelled.

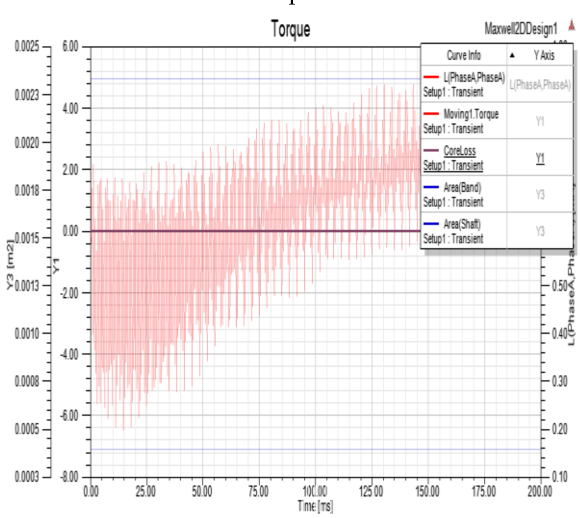


Figure 21. SIMULATED MOTOR CORE LOSES

Figure 22. presents optimized motor speed, when the selected three phase induction motor was modeled in

Ansys Maxwell, the speed was determined with respect to the time taken, then to optimize it for transport applications, the MATLAB tools were used. The objective 1 and objective 2 represents the selected motor speed and time taken. Here, the speed was diagonally corresponding to the time taken as well as the distance covered. In practice, this modeled three phase induction motor can withstand long distance transport use.

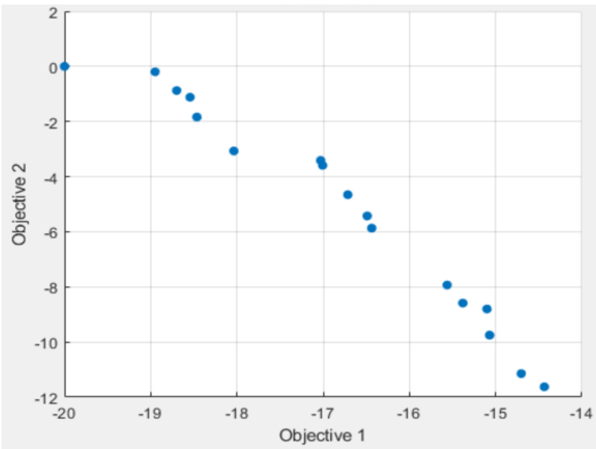


Figure 22. OPTIMIZED MOTOR SPEED

Figure 23. presents optimized frequency, it showed the response of the selected three phase induction motor frequency when it has been optimized. A corresponding maximum value of 40Hz at objective 1 to maximum value of 20sec in objective 2, showed the progressive phase of motor frequency when optimized and made suitable for transport applications.

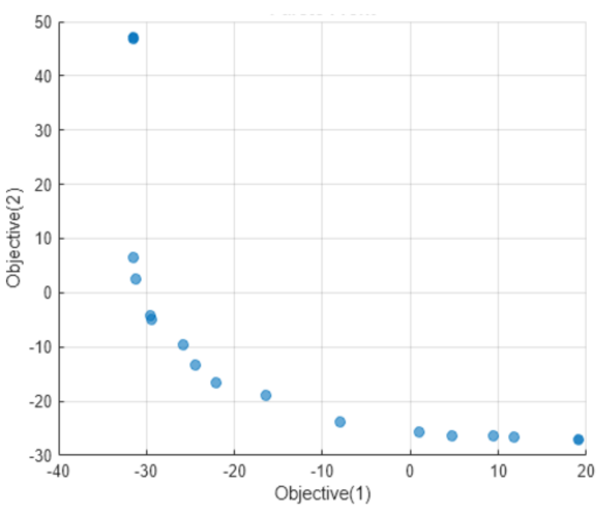


Figure 23. OPTIMIZED FREQUENCY

Figure 24. presents results of optimized torque, it showed the response of the selected three phase induction motor torque when it has been optimized. A corresponding maximum value of 5N-m at objective 1 to maximum value of 10sec in objective 2, showed the progressive phase of motor torque when optimized and made suitable for transport applications.

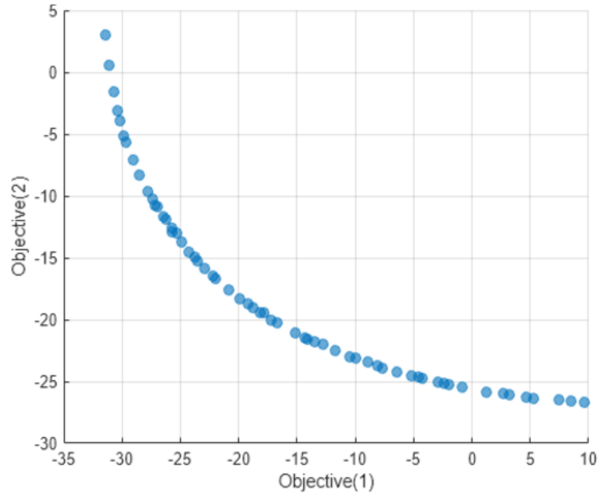


Figure 24. OPTIMIZED TORQUE

## Conclusions

This research project delves into the design and optimization of three-phase induction motors (IMs) specifically tailored for transport applications. The primary objective is to enhance the efficiency, power density, and overall performance of these motors while minimizing material usage and production costs. The research successfully demonstrates the effectiveness of a multi-objective optimization approach in designing high-performance induction motors for transport applications. By carefully considering the trade-offs between efficiency, power density, and cost, the optimized designs offer significant improvements over conventional designs. The FEA simulations provide valuable insights into the electromagnetic and thermal characteristics of the motor, enabling fine-tuning of the design parameters to achieve optimal performance. The use of advanced optimization techniques ensures that the design process is efficient and robust.

## *References*


[82] Bose, R., Gupta, N., and Mehta, P. 2022. Predicting electrical load demand in smart grids using neural networks in MATLAB. Energy Informatics Journal, 10(1), 122-134.

[83] Chen, L., and Zhao, F. 2019. Thermal management challenges in three-phase induction motors for transportation. IEEE Transactions on Energy Conversion, 34(6), 987–995. https://doi.org/10.1109/TEC.2019.02.007

[84] Chen, W., and Li, X. 2022. Optimization of chemical reactor operations using MATLAB. Industrial and Chemical Engineering Research, 61(2), 78-89.

[85] Johnson, P., and Lee, H. 2019. Regenerative braking systems in electric buses using induction motors. IEEE Transactions on Vehicular Technology, 68(4), 2890-2901.

[86] Kumar, P., Singh, A., and Roy, V. 2020. Optimization techniques for improving induction motor efficiency in transport applications. Advances in Electrical Engineering, 78(5), 567–579. https://doi.org/10.1016/ade.2020.567

[87] Kumar, R., Singh, V., and Patel, P. 2020. Electromagnetic design optimization of three-phase induction motors using finite element analysis. International Journal of Electrical Power and Energy Systems, 117, 105621.

[88] Rao, S., Kumar, A., and Verma, R. 2022. Energy-efficient motor designs for electric buses using ANSYS Maxwell. Renewable Energy Journal, 37(4), 435-448.

[89] Smith, J., and Johnson, K. 2020. Design considerations for three-phase induction motors in automotive applications. International Journal of Electrical Systems, 12(4), 211–225. https://doi.org/10.1109/IJES.2020.04.002

[90] Williams, M. 2022. The role of advanced materials in sustainable motor design for electric vehicles. Materials Science Advances, 56(1), 112–124. https://doi.org/10.1234/msa.2022.01.011